Remote Sensing of Environment 113 (2009) 2560–2573

Contents lists available at ScienceDirect

Remote Sensing of Environment

journal homepage: www.elsevier.com/locate/rse

A dorsiventral leaf radiative transfer model: Development, validation and improved model inversion techniques

Jan Stuckens [a,*], Willem W. Verstraeten [a], Stephanie Delalieux [b], Rony Swennen [c], Pol Coppin [a]

[a] Katholieke Universiteit Leuven, Biosystems department, M3-Biores, Willem de Croylaan 34, BE-3001 Heverlee, Belgium
[b] Flemish Institute for Technological Research (VITO), Center for Remote Sensing and Earth Observation Processes (TAP) Boeretang 200, BE-2400 Mol, Belgium
[c] Katholieke Universiteit Leuven, Biosystems Department, Division of Crop Biotechnics, K.U. Leuven, Kasteelpark Arenberg 13, BE-3001 Heverlee, Belgium

ARTICLE INFO

Article history:
Received 1 December 2008
Received in revised form 18 July 2009
Accepted 18 July 2009

Keywords:
Leaf optical properties
Asymmetry
Radiative transfer
Absorption
Scattering
Pigments

ABSTRACT

A Dorsiventral Leaf Model (DLM) is presented to simulate leaf radiative transfer. DLM was conceived as a plate model with a stochastic distribution of different groups of layers. Leaf asymmetry was modeled by assigning non-uniform distributions of pigments, water and dry matter to palisade and mesophyll layers and by simulating different amounts of light diffusion for adaxially and abaxially incident light. Surface reflections are based on micro-facets theory enabling the simulation of directional–hemispherical reflectance and a range of bidirectional reflectance factors. Adaxial and abaxial optical properties could be accurately simulated for a variety of leaf types with an overall error in reflectance and transmittance below 1.3%. Sensitivity analysis focused on optimizing model inversion schemes improves parameter estimation accuracy. Different inversion schemes were compared for two independent datasets. Results underpin most of the propositions of the sensitivity analysis: (i) masking the near-infrared wavelengths (band weighting) to account for variability in the dry matter composition consistently increased predicted accuracies for dry matter content, (ii) white reflectance measurements (reflectance with a 100% diffusely reflecting background) provided results superior to other optical measurements, making it a valuable and fast alternative and (iii) combining reflectance and transmittance into absorptance however did not result in improvements. Comparisons of DLM with the PROSPECT 5 model indicate an almost equal performance in content estimations. Improvements were thus not related to differences in model structure but to techniques that reduce the impact of leaf structure and compensate for sampling errors and variations in specific absorption spectra. DLM has important potential in the study of leaf radiative transfer and in the integration with canopy radiative transfer models.

1. Introduction

Leaf optical properties have been recognized as key variables in the description and modeling of radiative transfer in canopies. The interaction of electromagnetic radiation with leaves, resulting in reflection, transmission, absorption and fluorescence, depends on their chemical and physical characteristics (Allen et al., 1969, 1970; Jacquemoud & Baret, 1990). In modeling leaf optical properties in the 400–2500 nm range, a wide variety of radiative transfer models exist. They are classified by Jacquemoud and Ustin (2001) in increasing order of complexity into plate models (of which the PROSPECT model of Jacquemoud and Baret (1990) is the best known example), N-flux models, stochastic models, models based on the radiative transfer equation and ray tracing models. Models of each class have been used to obtain accurate and coherent simulation of reflectance and transmittance of broad-leaved and needle-shaped leaves.

Major factors impacting the scientific success of existing models, in no specific order, are the model's validation, the ability to invert the model, its integration with canopy radiative transfer models, the availability of the model to the scientific community and the model's complexity.

Recent research has focused on modeling of the leaf bidirectional reflectance distribution function (BRDF) (Bousquet et al., 2005), modeling of fluorescence (Zarco-Tejada et al., 2006) and the possibility of separating pigments such as carotenoids and chlorophyll a versus b (Feret et al., 2008). Attempts to apply inversion techniques of leaf radiative transfer models to separate different components of leaf dry mass such as lignin, cellulose and sugars on fresh leaf spectra were largely unsuccessful (Fourty et al., 1996), although statistical approaches proved successful for dry and – to some extent – for fresh material (Jacquemoud et al., 1995).

The impact of leaf internal structure on its optical properties has been subject to extensive research. The differences in optical properties of dorsiventral (also called bi-facial or asymmetric) leaves have been well described. Woolley (1971) reports higher directional hemispherical reflectance of abaxial soybean faces than of adaxial

* Corresponding author. Tel.: +32 16 32 97 49.
E-mail address: Jan.Stuckens@biw.kuleuven.be (J. Stuckens).

0034-4257/$ – see front matter © 2009 Elsevier Inc. All rights reserved.
doi:10.1016/j.rse.2009.07.014

faces for most of the 400–2700 nm spectrum, but an inversion of this effect in the near infrared (NIR, 800–1300 nm). Directional hemispherical transmittance of the abaxial face in the NIR was found to be higher than of the adaxial side. Analogous results were described in Baldini et al. (1997). Different models have been developed that account for the dorsiventral structure of leaves. Yamada and Fujimura (1991) developed a four layer reflectance and transmittance model based on Kubelka–Munk theory and subsequently applied this model to predict chlorophyll content. Richter and Fukshansky (1996) developed and extended a four-flux radiative transfer model for predicting radiation fluxes inside a leaf using optical microprobe measurements for calibration. Ma et al. (2007) extended PROSPECT into the dorsiventral model QSPECT that counts four layers: adaxial epidermis, palisade mesophyll, spongy mesophyll and abaxial epidermis. Each layer's optical properties were calculated with the PROSPECT model with different values for biochemical content and structure. In addition, leaf optical properties have also been simulated using Monte Carlo sampling: Govaerts et al. (1996) developed the ray-tracing model RAYTRAN to simulate photon transport in a 3D dorsiventral leaf and Baranoski (2006) developed an Algorithmic Bidirectional surface scattering Model for Bi-facial leaves (ABM-B) that uses random walk Monte Carlo sampling to compute optical properties. The influence of leaf asymmetry into the model's structure on the retrieval of biochemical properties (model accuracy and bias) has hitherto not been assessed. A precise modeling of both adaxial and abaxial optical properties for broadleaved species is of importance in remote sensing research since research provided evidence that ignoring differences between both faces may introduce significant errors in the simulation of canopy reflectance (Stuckens et al., 2009). While aforementioned research focused on broad-leaved species, (Dawson et al., 1998) were able to construct a model that simulated optical properties of fresh and dried needle-shaped leaves.

Model inversion problems of either leaf or canopy radiative transfer models are most often tackled by least squares minimization or table look-up approaches. Both unconstrained and constrained (e.g. (Kuusk, 1991) who uses a penalty term for unrealistic parameter values) minimizations are applied. Least squares minimization relies on important assumptions: the errors between wavebands have to be uncorrelated with each other and with the independent variables and have equal variance (Bjõrck, 1996). As these assumptions are rarely met in hyperspectral remote sensing it can be expected that more successful inversion schemes can be designed by using band weighting, alternative definitions of independent variables (spectra) or neural networks (e.g. Atzberger, 2004; Bacour et al., 2006).

For leaf optical models further improvements in parameter prediction are expected by coherent improvements in the model's architecture (e.g. including asymmetry) and in inversion techniques. Additional improvements may be obtained by more accurate estimations of spectral constants such as specific absorption spectra. The first objective of this research is to develop and validate an algorithmically fast, invertible model for dorsiventral broad-leaved leaves that can be implemented in different types of canopy reflectance models. The second objective is to design an optimized measurement and inversion procedure that allows a more accurate prediction of biochemical contents.

The Materials and methods section describes the collection and properties of reference datasets that include spectral measurements and contents determination. The model description section presents an analysis of leaf anatomical structure that will be used as a template for a mathematical formulation of a dorsiventral leaf model (DLM). The interaction between model parameters and the consequences of model and measurement errors will be interpreted in the sensitivity analysis. The validation section investigates spectral approximation of measured spectra for both adaxial and abaxial reflectances and the accuracy of parameter estimations for different model inversion schemes.

2. Materials and methods

Three datasets were collected. The first dataset, LeuvenC, is a model calibration dataset consisting of 20 leaves from 12 different species for which adaxial and abaxial directional-hemispherical reflectance and transmittance were recorded in March 2009 with a RTS-3ZC integrating sphere (updated version) coupled to an ASD Fieldspec spectroradiometer (Analytical Spectral Devices, Boulder, Co) measuring from 350 to 2500 nm with a spectral resolution of 3 nm in the 350–1050 nm range and 10 nm in the 1050–2500 nm range. Sample holders were removed from the sphere to avoid reduced port reflectance errors. Scans of 5–10 s per leaf were taken from different positions and averaged. Leaves were kept on their stems during measurements to minimize water loss. Data were noise filtered with a zero phase forward and reverse fourth order Butterworth filter (Oppenheim & Schafer, 1989). From the same leaves, five 1 s scans were made with an ASD leaf probe for instrument intercomparison. The leaf probe measurement chamber has an incandescent light source with illumination perpendicular to the leaf and a viewing angle centered at 40°, measuring biconical reflectance (Schaepman-Strub et al., 2006). Given the limited solid viewing and illumination angles it will further be approximated by bidirectional reflectance. All spectra were corrected to absolute reflectance using the manufacturer provided reflectances of the Spectralon (Labsphere, USA) white-panels. Additionally an intercalibration between the whitepanels of the integrating sphere and leaf probe was established. Intercompatibility of both measurement types for modeling purposes is theoretically treated in Section 4.3 and tested in Section 6.1.

A validation dataset (LeuvenV) was collected in June 2008 consisting of coupled measurements of optical properties and leaf biochemistry for 107 leaves of 10 species with varying leaf structure: *Citrus sinensis* L. (orange), *Malus domestica* Borkh. (apple), *Prunus avium* L. (sweet cherry), *Zea mais* (corn), *Solanum tuberosum* L. (potato), *Musa* sp. (banana), *Populus* × *canadensis* (poplar), *Fagus sylvatica* L. (beech), *Acer pseudoplatanus* (Norway maple) and *Euonymus fortunei* (albino leaves of a variegated cultivar). Leaf samples were taken in and spectral and biochemical analysis were made on the day of sample collection. No indications of senescence were present in the samples. Sealed plastic bags and refrigerator storage were used to prevent intermediate dehydration. Spectral measurements were made with an ASD spectroradiometer and a leaf probe. For each leaf, two measurements were made of adaxial and abaxial reflectance using a matte plastic background with a flat reflectance spectrum of 4%. The effect of the background on reflectance measurements was included into the model structure as described in Section 4.8. An additional pair of measurements was made of the adaxial reflectance with the same Spectralon whitepanel as a background, hereafter called 'white (adaxial) reflectance'. This spectral measurement set comprises a fast method (1 s scan time per measurement) that can easily be adapted to field work. Per leaf, dry mass and water contents were determined by weighting three up to five fixed area (2.4 cm^2) tissue disks in fresh state and after drying at 85 °C in an oven for at least 16 h. In additional drying experiments, the difference in measured water content between 16 h and a four days extended drying period was below 0.04 mg/cm^2, which is one order of magnitude smaller than the accuracies obtained in this research. Chlorophyll a and b and carotenoids were determined on five tissue samples of 0.79 cm^2 by absorption spectroscopy using an UV–VIS Perkin Elmer Lambda 12 spectrophotometer and an acetone–Tris extraction solvent. Contents were calculated using the equations described by Sims and Gamon (2002) which includes a correction for the absorption by anthocyanins. These authors report the accuracy of their method when compared to High Performance Liquid Chromatography (HPLC) pigment determinations with a coefficient of determination (R^2) of 0.96 for chlorophylls.

As a third dataset, the LOPEX dataset (Hosgood et al., 1994) was used which contains a larger number of biochemical properties and

leaf reflectance and transmittance spectra of 60 broad-leaved species. As reported by Feret et al. (2008), the pigment contents in LOPEX are questionable possibly due to inefficient pigment extraction procedures. Accuracies on LOPEX chlorophyll content estimation are included in the analysis to facilitate comparison with other published results but should be treated with care. Table 1 summarizes relevant properties of the LeuvenV and LOPEX datasets.

3. Analysis of abaxial and adaxial optical properties

Fig. 1 shows the structure of a dorsiventral leaf, typical for most broad-leaved dicot species. The palisade mesophyll layer consists of densely packed cells with few intercellular spaces. The underlying spongy mesophyll is loosely packed with large intercellular spaces. The adaxial (top) and abaxial (bottom) sides of the leaf are bound by an epidermal layer with a cuticle of varying thickness. Quantification studies in sun-lit and shade leaves of *Spinacia oleracea* (Cui et al., 1991) and *Acer platanoides* (McCain et al., 1993) reveal that the highest chloroplast concentrations are found in the palisade tissue, with lower concentrations in the spongy tissue and almost no chloroplast concentrations in the epidermal layers.

Fig. 2 shows typical directional–hemispherical reflectance and transmittance spectra of the adaxial and abaxial sides of two leaves, *Urtica dioica* L. (nettle) and *Hedera helix* L. (ivy) with different dorsiventral structures. Marked differences between adaxial and abaxial optical properties exist (i) in the VIS region (400–700 nm) where abaxial reflectance exceeds adaxial reflectance with approximately equal transmittances, (ii) in the NIR region (700–1400 nm), where the adaxial reflectance is higher and the adaxial transmittance is lower and (iii) in the SWIR region (1400–2500 nm) where abaxial reflectance is higher in the water absorption bands and both positive and negative differences are found in the 1600–1800 and 2000–2400 nm regions. In addition, Baldini et al. (1997) report additional reflectance and transmittance plots between 400 and 1100 nm from which similar conclusions can be drawn. An important observation from Fig. 2, which confirms observations by Woolley (1971) and Baldini et al. (1997) is that the (NIR) transmittance of the abaxial side is systematically higher than on the adaxial side. This observation is in seeming conflict with the reciprocity relation (or polarity property) for transmitted light (Kubelka, 1954) which states that scattering and absorption are unaffected when the path of light is exactly reversed. For a directional–hemispherical configuration this implicates that at the opposite face of the leaf the hemispherical–directional transmittance is measured, under the same zenith angle. This is not applicable

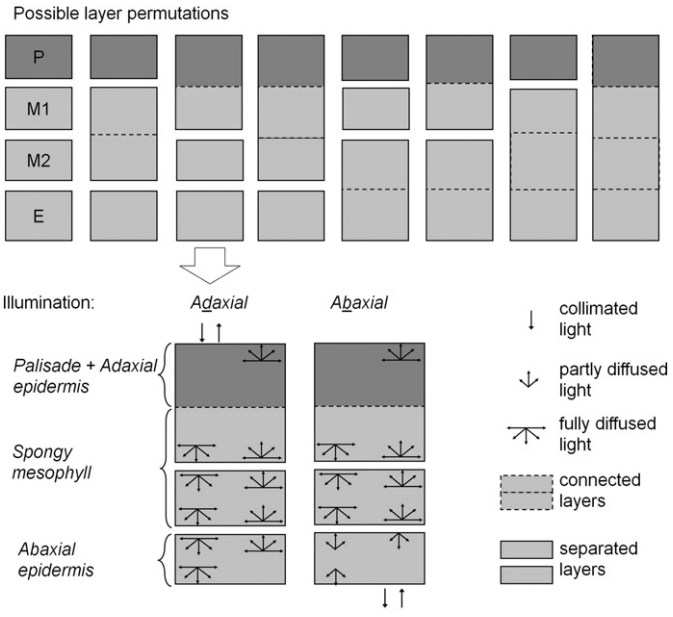

Fig. 1. Structure of a typical dorsiventral leaf.

to our model and measurements that consider a directional–hemispherical configuration at both faces. As a consequence differences in transmittance from both faces of a surface are physically plausible and should not be attributed to measurement errors.

Aforementioned observations can be explained by considering the cross-section of a dorsiventral leaf:

1. The compact structure of the palisade layer was found to facilitate penetration of adaxial light into the spongy tissue (Vogelmann & Martin, 1993), where the light is scattered due to the large amount of cell–air interfaces of the more loosely packed cells. Elevated concentrations of chlorophyll in the palisade layer will further reinforce this effect. For abaxial illumination, the scattering by the spongy mesophyll cells occurs before light can be guided into the leaf interior, which increases the reflectance.
2. The difference between adaxial and abaxial directional–hemispherical transmittance can be explained by representing a leaf as a stack of 'optical' layers separated by air spaces (Fig. 1). The adaxial epidermis and palisade tissue are connected over most of their surface with almost no intercellular spaces and are therefore be represented by a

Table 1
Characteristics of the datasets.

	Dataset	Leuven	LOPEX
	Year	2008	1993
	Number of samples	107	64 (pigments)/330 (water and dry matter)
	Number of species	10	50
	Instrument	ASD FieldSpec FR	Perkin Elmer Lambda 19
	Spectral range	400–2500 nm	400–2500 nm
	Solvent	Acetone 80% w. Tris buffer (pH 7.8)	Acetone 100%
	Pigment extraction method	Sims and Gamon (2002)	Lichtenthaler (1987)
Total chlorophyll (g/cm^2)	Min	0.4	0.5
	Max	113.8	72.6
	Mean	39.2	20
Carotenoids (g/cm^2)	Min	0.3	0.6
	Max	8.5	15.8
	Mean	22.2	4.4
Water (mg/cm^2)	Min	3.9	4.3
	Max	41.2	43.9
	Mean	13.7	11.3
Dry matter (mg/cm^2)	Min	1.8	1.7
	Max	12	15.2
	Mean	6.2	5.3

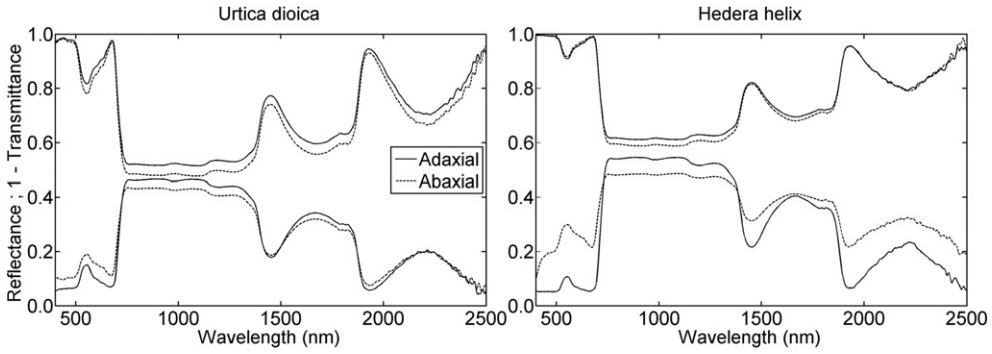

Fig. 2. Reflectance and transmittance of abaxial an adaxial faces of *Urtica dioica* and *Hedera helix*.

single optical layer of which the mesophyll tissue causes light scattering (Vogelmann & Martin, 1993). The abaxial epidermis is disconnected from the spongy tissue over a large fraction of its surface and is therefore expected to optically function as a separate layer. The generally smooth oblate shape of epidermal tissue (Baranoski, 2006; Taiz & Zeiger, 2006) is expected to cause low amounts of scattering and even focusing of light (Vogelmann et al., 1996). Abaxial collimated light is thus not fully diffused upon entering the abaxial epidermis (bottom layer) but only upon entering the spongy tissue (middle layers) while adaxial collimated light is immediately diffused by the top optical layer. As a consequence, abaxial transmittance can be higher than adaxial transmittance due to the lower total amount of light scattering.

3. The effects in the SWIR region can be considered as a mixture of the previous items, with the concentration effect dominating in high absorption regions and the dispersion effect dominating in low absorption regions.

In the following sections, an analytical Dorsiventral Leaf Model (DLM) is developed that takes into account the described asymmetric behavior of light scattering and absorption.

4. Model description

DLM is based on the well known plate generalized model (Allen et al., 1970) that simulates reflectance and transmittance of leaves represented by a set of horizontal layers separated by air spaces. First, the adaxial and abaxial optical properties of a single layer are determined for a generalized case of partly diffused light. Next, the optical properties of a stack of non-identical layers is derived. For the top layer on which light is incident, the model formulation is extended to either directional–hemispherical reflectance (DHR) and transmittance (DHT) or bidirectional reflectance factor (BRF) (Schaepman-Strub et al., 2006). In the subsequent sections, default model parameters are established, the refractive index of cell walls is re-calibrated and the plate model is extended to calculate leaf reflectance with a background of known reflectance.

4.1. Reflectance and transmittance of a single layer

Reflectance and transmittance of a single layer in DLM are a generalization of the formulation derived in Jacquemoud and Baret (1990), for conditions where light inside a layer is not necessarily fully diffused. Consider a layer illuminated by either a collimated or diffuse light source. The layer's hemispherical reflectance and transmittance are derived from the average of the Fresnel transmission coefficients (t) at the air-to-cell and cell-to-air interfaces and the average transmissivity (τ) of light passing through it. The value of t depends on the maximum dispersion angle of the light (α for light outside of the layer and $\tilde{\alpha}$ for light inside the layer), the relative refractive index of the layer (η) and the direction in which light crosses the interface. An analytical formulation is given in Allen et al. (1969). We will use t_o for light entering a layer (air-to-cell interface) and t_i for light leaving the layer (cell-to-air interface). The angular distribution of incident light may be different for both faces of a layer, so α and $\tilde{\alpha}$ depend on the direction of illumination (z), which is abaxial ($z='b'$) or adaxial ($z='d'$). The average transmissivity $\tau(\tilde{\alpha},k)$ is found by averaging the Beer–Lambert law over $\tilde{\alpha}$:

$$\tau(\tilde{\alpha},k) = \frac{\int_0^{\tilde{\alpha}} e^{-k/\cos(\theta)}\cos\theta\sin\theta\,d\theta}{\int_0^{\tilde{\alpha}}\cos\theta\sin\theta\,d\theta} = \frac{1}{1-\cos^2\tilde{\alpha}}\left[e^{-k}(1-k)+e^{-k/\cos\tilde{\alpha}}\cos\tilde{\alpha}(k-\cos\tilde{\alpha})+E_1(k)-E_1\left(\frac{k}{\cos\tilde{\alpha}}\right)\right] \quad (1)$$

where k is the absorption coefficient of a layer and E_1 stands for the exponential integral (for a mathematical proof, see online documentation). For $\tilde{\alpha}=90$ the formula simplifies to the version used in Jacquemoud and Baret (1990). The reflectance (R_z) and transmittance (T_z) of a layer with light incident from direction z can now be expressed as:

$$R_z = R_s + \frac{T_s\tau(\widetilde{\alpha_z},k)^2 t_i(\widetilde{\alpha_z},\eta)(1-t_i(\widetilde{\alpha_z},\eta))}{1-\tau(\widetilde{\alpha_z},k)(1-t_i(\widetilde{\alpha_z},\eta))^2}$$
$$T_z = \frac{T_s\tau(\widetilde{\alpha_z},k)t_i(\widetilde{\alpha_z},\eta)}{1-\tau(\widetilde{\alpha_z},k)(1-t_i(\widetilde{\alpha_z},\eta))^2} \quad (2)$$

with R_s the surface reflectance and T_s the surface (hemispherical) transmittance of the layer (see Section 4.3). For leaf internal scattering (all layers except the top layer), we will use Allen's approximation where $T_s=t_o(\alpha_z,\eta)$ and $R_s=1-T_s$. For the top layer a more detailed treatment is presented in Section 4.3. The reflectance and transmittance of a layer illuminated by either adaxial or abaxial sides will be represented by a four element vector: $[R_{z=d}, T_{z=d}, R_{z=b}, T_{z=b}]$.

4.2. Reflectance and transmittance of a group of layers

In calculating the reflectance and transmittance of a group of homogeneous layers, Jacquemoud and Baret (1990) extended the 'generalized plate model'. In this symmetric model, abaxial and adaxial optical properties are equal. This plate model theory is further improved here to model the asymmetry of dorsiventral leaves. A four-layer representation of a leaf (Fig. 3) was developed for DLM. The top layer (P) represents the aggregate of adaxial epidermis and palisade mesophyll. Both are assumed to optically represent a single layer, as motivated in Section 3) and will henceforth be simply named 'palisade layer'. This assumption agrees with the results of Ma et al. (2007) who treated the adaxial epidermis as a separate layer, but assigned to it a very low structure parameter. The second and third layers represent the spongy mesophyll (M_1 and M_2). The lower epidermis (E) is treated as a fourth layer since it is not always tightly connected to the spongy mesophyll (see Fig. 1 and Section 3). The

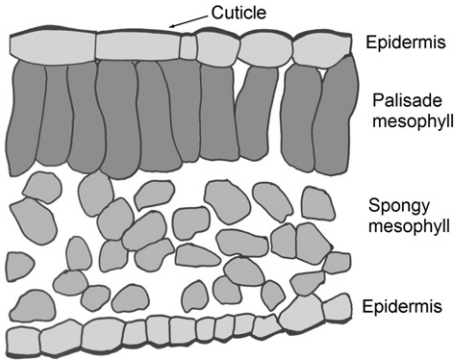

Fig. 3. Schematic structure of the Dorsiventral Leaf Model for three out of eight layer groups with adaxial and abaxial illumination. The bottom line shows the group probabilities.

choice of two spongy mesophyll layers and thus a four layer leaf representation has no direct physical basis, but was chosen as an upper bound in representing the (near-infrared) scattering behavior that is expected to be dominant in the spongy layers. Simulations with different model structures revealed that a four-layer leaf structure was sufficient to model the scattering of all leaves in the Leuven and LOPEX datasets while a three layer representation was insufficient for thicker leaves.

Contrary to the traditional interpretation of layers in plate models, in DLM two adjacent layers are separated by air spaces for only a fraction (f_{air}) of their surface area and are connected for the remainder fraction ($1-f_{air}$). The parameter f_{air} determines the scattering behavior and is analogous to the structure parameter N in the PROSPECT model. It is equal for each pair of adjacent layers. The adaxial and abaxial reflectance and transmittance of two adjacent layers (A and B) for the area over which they are separated by air spaces, can be given in the four-element notation:

$$\left[R_{AB,d}, T_{AB,d}, R_{AB,b}, T_{AB,b}\right] = \left[R_{A,d} + \frac{T_{A,d}R_{B,d}T_{A,b}}{1-R_{A,b}R_{B,d}};\ \frac{T_{A,d}T_{A,d}}{1-R_{A,b}R_{B,d}};\ R_{B,b} + \frac{T_{B,b}R_{A,b}T_{B,d}}{1-R_{A,b}R_{B,d}};\ \frac{T_{B,b}T_{B,b}}{1-R_{A,b}R_{B,d}}\right] \quad (3)$$

The fractional area over which A and B are connected (no air spaces) on the other hand, can be represented by a single layer with a layer absorption coefficient $k_{AB}=k_A+k_B$. The above formulas for two layers can be iteratively applied to find reflectance and transmittance of three and finally four layers. The reflectance and transmittance of an entire leaf consists of a combination of reflectances and transmittances of the eight possible permutations in which four layers can either be separated or connected: [$P.M_1.M_2.E$]; [$PM_1.M_2.E$]; [$P.M_1M_2.E$]; [$P.M_1.M_2E$]; [$PM_1M_2.E$]; [$P.M_1M_2E$]; [$PM_1.M_2E$]; [PM_1M_2E]. In this notation a dot indicates separation by air spacing and connected letters indicate connected layers. The upper part of Fig. 3 visualizes these combinations, while the lower part illustrates a detail of a single permutation ([$PM_1.M_2.E$]). The total leaf reflectance and transmittance (RT_{leaf}) is then a weighted average of the reflectances and transmittances of the individual permutations (RT_i):

$$RT_{leaf} = \sum_{i=1}^{8}(w_i RT_i) \quad (4)$$

with the weights given as $w_i = f_{air}^{n} f_{air}^{3-n}$ where n equals the number of air layers (number of dots) in the permutation. The eight weights form a binomial distribution and sum up to one so no normalization is required.

4.3. Reflectance of the top layer

In this section we will derive expressions for BRF and DHR of leaf surfaces for implementation in DLM. BRDF modeling of leaf surfaces has been subject to research in domains of computer graphics (e.g. Habel et al., 2007) and remote sensing (Bousquet et al., 2005; Govaerts et al., 1996). Surface reflectance is derived from the Bousquet micro-facets model (calibrated on beech, laurel and hazel leaves) and allows an intercompatibility relationship to be established between DHR and BRF of leaf surfaces. The leaf BRDF in Bousquet's model is represented as the sum of a diffuse component ($BRDF_d$) representing the leaf interior absorption and scattering and a glossy/specular component ($BRDF_s$) related to the cuticle surface reflectance: $BRDF = BRDF_s + BRDF_d$. This formulation is not directly compatible with plate models (Eq. (2)) and does not assure energy conservation (Ashikhmin & Shirley, 2000) as it does not account for Fresnel-based reduced reflectance i.e. light reflected off a surface does not enter the leaf interior and does not contribute to diffuse reflectance. The previous equation is therefore extended to: $BRDF = BRDF_s + (1-DHR_s)BRDF_d$ where DHR_s is the directional–hemispherical surface reflectance obtained by hemispherical integration of $BRDF_s$. $BRDF_s$ is calculated using the Cook and Torrance (1981) model:

$$BRDF_s(\eta(\lambda), \theta_s, \theta_v, \varphi_v, \sigma) = \frac{Fr(\eta(\lambda), \theta_a) D(\alpha, \sigma) G(\theta_s, \theta_v, \varphi_v)}{4\cos\theta_s \cos\theta_v} c \quad (5)$$

with λ the wavelength, θ_s the light incident angle, θ_v the viewing angle, φ_v the relative azimuth, $\eta(\lambda)$ the refractive index of the cuticle that is assumed to be equal to cell walls, θ_a the half-angle between illumination and viewing directions, α the angle of the facets normals, σ a surface roughness parameter, Fr the Fresnel reflectance, D a (normalized) micro-facets distribution function, G a shadowing term and c a normalization constant. Of these terms only the Fresnel term depends on wavelength (λ).

For implementation in DLM we restrict calculations to collimated light incident perpendicular to the leaf surface ($\theta_s=0$) and viewing angles between 0 and 45° ($\theta_a<22.5°$) which conforms with optical designs of commonly used measurement instruments such as leaf probes and integrating spheres. Under such conditions it can be derived (see online documentation) that $\theta_a=\alpha=\theta_v/2$, $BRDFs$ no longer depends on φ_v and the Fresnel reflectance almost equals the Fresnel reflectance at normal incidence: $Fr(\eta,\theta_a)\approx Fr(\eta,0)$ (relative error<1%). The BRF_s (equal to $\pi BRDF_s$) can be closely approximated by the product of two separate terms: the Fresnel factor and a wavelength-independent term (ν) that depends on viewing geometry and surface roughness:

$$BRF_s(\eta(\lambda), \theta_v, \sigma) \approx m(\theta_v, \sigma) Fr(\eta(\lambda), 0);\ \theta_v < 45^{o} \quad (6)$$

Monte Carlo simulations on the Bousquet micro-facets model with a wide range of refractive indices (between 1.1 and 1.6) and surface roughnesses (between 0.2 and 1) show that errors of this approximation were below 10^{-4} for $\theta_v<45°$ (see online documentation). In a second Monte Carlo experiment equal accuracy standards were obtained for the DHR_s so that:

$$DHR_s(\eta(\lambda), \sigma) \approx \mu(\sigma) Fr(\eta(\lambda), 0) \quad (7)$$

with μ a different constant that only depends on surface roughness. Now the values of R_s and T_s of Eq. (2) can be determined. For DHR simulations, $R_s=DHR_s$ and $T_s=1-DHR_s$ and for BRF simulations, $R_s=BRF$ and $T_s=1-DHR_s$ since T_s stands for hemispherical transmittance in both cases. BRF and DHR for these conditions only differ in their specular components and the difference between both is independent of biochemical content or leaf internal scattering. While DHR can be measured with an integrating sphere, derivations made for BRF can be

ported, without loss of accuracy, to biconical reflectance (e.g. measured with a leaf probe) since this integrates bidirectional reflectance over viewing and illumination directions (Schaepman-Strub et al., 2006).

4.4. Model parameters

The absorption coefficients (k) of the palisade and spongy mesophyll layers and the abaxial epidermis are expressed as linear combinations of the different layer biochemical contents (in mass per unit area) with their respective specific absorption spectra ($\kappa(\lambda)$ in unit area per mass). Further analysis will be restricted to the four main components of a leaf's biochemical composition (Fourty et al., 1996; Feret et al., 2008): total chlorophyll a + b (C_{chl}), total carotenoids (C_{car}), water (C_{wat}) and total dry matter (C_{dm}). For easier parametrization the following generalizations are made: (i) water and dry matter contents in each layer are present in equal proportions with respect to the total leaf contents, (ii) the chlorophyll and carotenoids contents in each layer are also present in equal proportions, (iii) the biochemical contents in the spongy mesophyll layers are equal and (iv) the adaxial epidermis contains a reduced chlorophyll content (only in stomatal cells; (Taiz & Zeiger, 2006)). The absorption coefficient of each layer can now be found for known values of these four components and the fractions of the total pigment content (β_{pigm}) and water and dry matter content (β_{wdm}) in the palisade layer and the fraction of pigments in the abaxial epidermis (β_{ep}).

The arrows on the bottom drawing of Fig. 3 show the scattering of light between the different layers. Light incident upon a leaf is collimated with normal incidence. Leaf surface roughness is modeled as described in Section 4.3 and parametrized by μ for DHR and by μ and ν for BRF. Adaxially incident light is assumed to be diffused inside the palisade layer so that $\widetilde{\alpha_d} = 90^o$ for all layers. The abaxial epidermis on the other hand is expected to cause only partial light diffusion ($\widetilde{\alpha_b} = \delta$; $\delta < 90°$) considering its relative smoothness, light focusing and optical thinness of the epidermal tissue (Section 3). After crossing the first cell–air boundary light will become fully diffuse ($\widetilde{\alpha_b} = 90°$), as is the light in intercellular air spaces ($\alpha_d = \alpha_b = 90°$). Fully and partly diffused light beams are indicated in Fig. 3. An important consequence of different values for $\widetilde{\alpha_b}$ and $\widetilde{\alpha_d}$ inside a single layer is that the layer and overall leaf directional–hemispherical transmittance can be different for abaxial and adaxial illumination.

Since the refractive index spectrum ($\eta(\lambda)$) and the specific absorption spectra of the leaf components ($\kappa(\lambda)$) are treated as optical constants, the leaf optical properties can be represented by the following parameters: C_{chl}, C_{car}, C_{wat}, C_{dm}, β_{pigm}, β_{wdm}, β_{ep}, f_{air}, μ, ν and δ.

4.5. Default leaf asymmetry and roughness parameters

Since a total number of 11 parameters is expected to decrease the performance of inversion algorithms, causing them to become ill-posed, default average values are determined for the asymmetry parameters β_{pigm}, β_{wdm} and β_{ep} and for the leaf roughness parameter μ. This allows choosing between inversion schemes in which these parameters are either fixed or free (estimated by the inversion algorithm). Knapp et al. (1988) report more than 50% of the chlorophyll content in the upper 270–300 μm of a leaf cross-section with a 400 μm palisade layer thickness. Measurements of paradermal sections made by McCain et al. (1993) reveal approximately 67% of the leaf chlorophyll in the palisade layer, 31% in the spongy tissue and 4% in both epidermal layers together. Estimates of fractional mass in different layers can be obtained from measurements of intercellular space volume and layer thickness in epidermal, spongy and palisade tissues. Values derived from Evans et al. (1996) on six different species range between 49 and 62% of leaf mass present in the upper epidermis and palisade tissue, while values derived from Pääkkönen et al. (1995) on fresh and aging Birch leaves range between 44% and 51%. Model inversion on directional–hemispherical abaxial and adaxial reflectance and transmittance leaves of the LeuvenC dataset return average values of 0.52 for β_{pigm} and 0.44 for β_{wdm} which is within the range of values reported in literature. Since DLM is an abstraction of leaf structure, its parameters should be treated as effective parameters (i.e. different from the true values they are supposed to represent but resulting in equal optical interactions). Therefore inverted values are preferred. Inverted values for β_{ep} (chlorophyll in lower epidermis) range between 7% and 25% with an average of 11%, which is relatively high. It may be assumed that the bottom layer effectively represents the abaxial epidermis and a fraction of the spongy tissue.

An average value for leaf roughness (μ) was estimated on the LOPEX dataset that consists of a larger number of directional–hemispherical adaxial reflectance measurements. A first estimate is based on model inversion (see Section 6) with μ as an additional free parameter, resulting in an average value of 1.19. A second estimate is based on the reflectance in the 400–450 nm range. Model calculations reveal that in leaves with moderate to high chlorophyll (>40 μg/cm^2) and carotenoid (>10 μg/cm^2) contents the diffuse part of the reflectance is less than 0.1% so that almost the entire reflectance is due to glossy reflections of the leaf cuticle. Using moderate or high chlorophyll and carotenoid contents as a selection criterion an average value of 1.14 was obtained, which is close to the previous estimate.

4.6. Specific absorption spectra

While the specific absorption coefficient of water has been directly measured (κ), the spectra of the other components have been determined by Jacquemoud and Baret (1990), Jacquemoud et al. (1996) and later by Feret et al. (2008) using model inversion. These spectra are being used in DLM, assuming that their shape is determined by the underlying physics, while their level (scaling) may be model-dependent.

4.7. Refractive index of cell walls

The refractive index spectrum of cell walls has been re-calibrated since its values were found to be significantly influenced by the difference in model structure between DLM and PROSPECT and more specifically by the assumptions of asymmetry. The calibration is made on 67 measurements of reflectance and transmittance of fresh leaves in the LOPEX dataset (five spectra averaged per species) for which ν (directional hemispherical) and δ (only adaxial) are not required. For each leaf C_{chl}, C_{car}, C_{wat}, C_{dm}, f_{air} and μ are determined from model inversions or measurements while fixed values (Section 4.5) are used for β_{pigm}, β_{wdm} and β_{ep} so that for each model layer, κ (Eq. (2)) can be found. The resulting values of $\eta(\lambda)$ were averaged resulting in the spectrum of Fig. 4. This spectrum significantly differs from values obtained by Feret et al. (2008) in their recalibration of the cell walls refractive index and its shape is closer to a monotonically decreasing line from approximately 1.5 at 400 nm down to 1.3 at 2500 nm. To evaluate whether these differences may be caused by differences in estimation procedures rather than by differences in model asymmetry, the procedure was repeated with parameter settings representing a perfectly symmetric leaf, analogous to the PROSPECT model (β_{pigm}, β_{wdm} and β_{ep} equal to 0.25). This result shows a shape similar to the spectrum of Feret et al. (2008). The effect of a symmetric model structure on the estimation of $\eta(\lambda)$ applied on dorsiventral leaves thus seems to cause a bias that is most pronounced in the 450–700, 1400–1550 and 1850–2000 nm wavelength ranges. A plausible cause is that at wavelengths of high absorption, most of the light entering a leaf is absorbed regardless of leaf asymmetry so that cuticular reflectance determines the estimated refractive index; at low absorption wavelengths, scattering dominates absorption so that biochemical content distributions (and thus asymmetry) have little

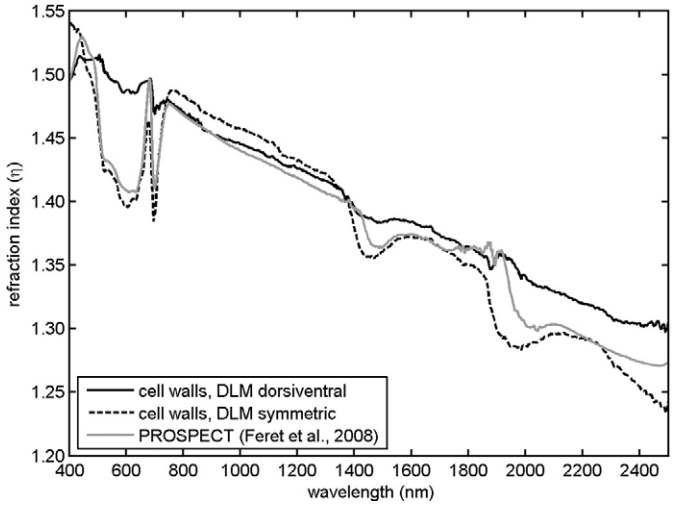

Fig. 4. Inverted spectra of the cell refraction index obtained from (i) DLM with a dorsiventral leaf assumption (ii) DLM with a symmetric leaf assumption and (iii) Feret et al. (2008).

effect; at zones of moderate absorption however, leaf reflectance and transmittance are more sensitive to biochemical content distributions and leaf asymmetry. The refractive index used in symmetric radiative transfer models such as PROSPECT is thus likely to be considered as an effective variable.

4.8. White reflectance and reflectance with a background

Inversion procedures for the estimation of biophysical content from optical measurements often require both reflectance and transmittance spectra. Different attempts have been made to replace both properties with one comprehensive measurement of which the concept of *infinite reflectance* (Allen et al., 1969; Lillesaeter, 1982) is the most widely known. It is defined as the reflectance of an optically thick stack of leaves, where the reflectance no longer increases with an increasing number of leaves. Even though infinite reflectance has important properties for the estimation of scattering and absorption coefficients and for the simulation of canopy reflectance, its practical use in the simulation of leaf optical properties is constrained by the requirement of a pile of almost identical leaves. An alternative and more convenient measure is the adaxial reflectance of leaves with a matte high reflective background (Lillesaeter, 1982), hereafter named *white (adaxial) reflectance* or R_{wh}. Using plate theory, white reflectance can be calculated for an asymmetric layer as:

$$R_{wh} = R_{d,c} + \frac{T_{d,c}T_{b,s}R_{wp}}{1 - R_{wp}R_{b,s}} \quad (8)$$

with $R_{d,c}$ and $T_{d,c}$ the adaxial reflectance and transmittance for collimated light, $R_{b,s}$ and $T_{b,s}$ the abaxial reflectance and transmittance of diffusely scattered light and R_{wp} the (absolute) reflectance of the whitepanel. White reflectance was combined with adaxial reflectance by Merzlyak et al. (2004) to estimate leaf transmittance. This procedure however required the additional assumptions that abaxial and adaxial reflectances and transmittances are equal and that differences between collimated and diffuse light can be ignored. Since this violates both our observations (Section 3) and our model structure and considering the significant errors produced by this estimation procedure, it was preferred here to directly measure and model white reflectance (see Section 2) rather than converting to transmittance. Important optical properties of white reflectance as an alternative to reflectance and transmittance are treated in the sensitivity analysis. Analogously to white adaxial reflectance, also white abaxial reflectance can be defined, but to reduce the total number of optical measures and inversion schemes being discussed in this text, this is not further discussed.

By replacing R_{wp} in Eq. (8) by the reflectance of any other (Lambertian) background, the reflectance of a leaf with different backgrounds can easily be calculated.

5. Sensitivity analysis

The sensitivity analysis is set up to provide more insights into the mechanisms that can cause random or systematic differences between predicted and measured biochemical variables. It breaks down into three modules. The first module assesses the sensitivity of simulated spectra to the model parameters. The second module focuses on the sensitivity to natural variability in a specific absorption spectra. The last module deals with the effects of sampling errors on model inversions.

5.1. Sensitivity of DLM to varying parameter values

The sensitivity of DLM was tested by evaluating differences in model output by the 11 parameters that drive the model. Model outputs considered here are adaxial and abaxial reflectance and transmittance, white reflectance and absorptance. The applied method is a variance based sensitivity analysis using the high dimensional model representation (HDMR) implementation developed by Ziehn et al. (2009). HDMR methods use a large number of randomly generated inputs (within operational parameter ranges) and their corresponding outputs to construct a high-dimensional Analysis of Variance (ANOVA) decomposition of the output dataset. The sensitivity of a parameter is often expressed by the Sobol' index (SI) (Sobol', 2001) that expresses the fraction of the total variance in a dataset explained by an individual parameter x_i (first order terms) or by the cooperative effect (interaction) of two parameters i and j: x_{ij} (second order terms). For a perfect high-dimensional representation, all first and second order terms sum up to one. Lower values indicate unexplained variance. A dataset of 2000 random parameters was generated with stochastic distributions of biochemical contents (C_{chl}, C_{car}, C_w and C_{dm}) derived from the LeuvenV and LOPEX datasets. The stochastic distributions of the seven structure parameters were estimated from initial model inversions of the LOPEX and LeuvenC datasets. For easier visualization the asymmetry effects (β_{pigm}, β_{wdm}, β_{ep} and δ) and BRDF effects (μ and ν) were grouped together. The second order terms of all interaction effects were relatively small and are represented as a single group. Fig. 5 shows the Sobol' indices per wavelength for adaxial and abaxial reflectance, absorptance and white reflectance. For all outputs the chlorophyll and water contents have a large impact on model sensitivity within their respective absorption regions. Dry matter content has a much smaller impact on adaxial and abaxial reflectance indicating that it may be significantly harder to retrieve with good accuracy. This agrees well with reported results of model inversions (Feret et al., 2008; Jacquemoud et al., 1996). Sensitivity to carotenoid content is low for all outputs, but abaxial reflectance and absorptance provide the highest sensitivity. Sensitivity to dry matter content of white reflectance and absorptance in contrast is far higher and dominates the NIR region. This indicates that use of either of both properties may result in more accurate content estimations. f_{air} has a large impact on adaxial and abaxial reflectance in the NIR and noticeable effects in the SWIR but almost no effect on white adaxial reflectance and absorptance. BRDF effects dominate the 400–500 nm region for most outputs and have small but noticeable effects in the higher wavelengths. Adaxial reflectance has a limited sensitivity to leaf asymmetry, mainly for wavelengths in the 1400–2500 nm range while abaxial reflectance is much more sensitive to leaf asymmetry over the entire spectrum. This may complicate the use of abaxial reflectance in content estimations. All outputs are to some extent sensitive to second order terms, which were found to be

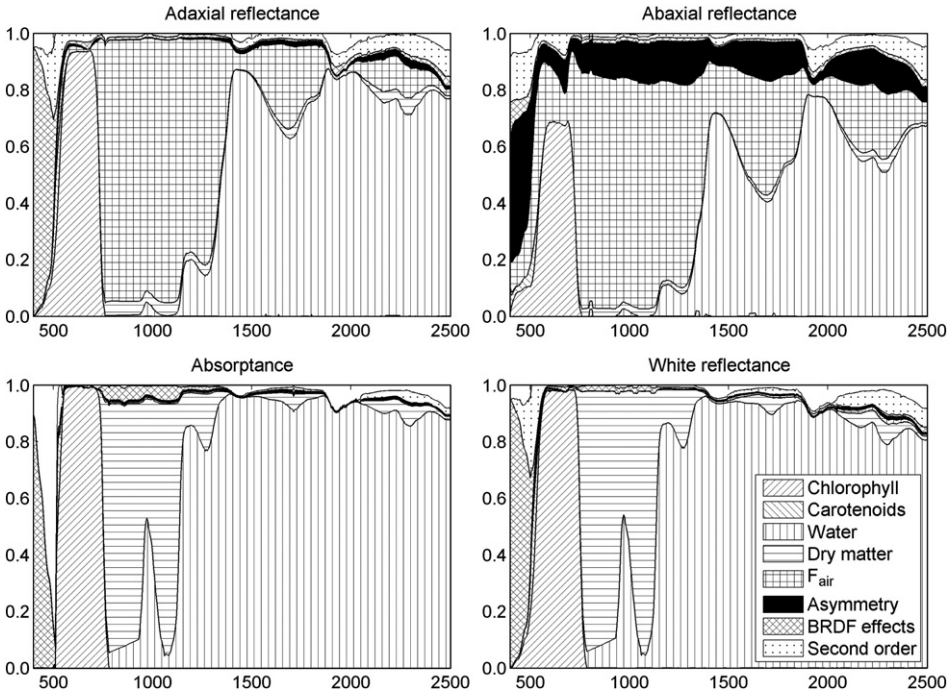

Fig. 5. Sobol' sensitivity index for individual and grouped model parameters and four different optical measures.

mainly composed of interactions between leaf structure and biochemical contents and interactions among biochemical contents (results not shown). For all outputs, a small fraction of the total variance (white part of the graphs) could not be explained by HDMR.

Both absorptance and white reflectance as alternatives to adaxial reflectance and transmittance may improve model inversions in applications where only content estimations (and not leaf structure) are targeted. Sensitivity is highly dependent on the input parameter ranges, which are derived here for fresh and relatively healthy (non-chlorotic) leaves of vegetations grown in temperate climatic conditions. Therefore generalization of these conclusions to other datasets including tropical, chlorotic or senescent leaves should be avoided.

5.2. Sensitivity to variations in specific absorption spectra

This section will focus on (inherent) variability in specific absorption spectra of dry matter and chlorophylls. For water, multiple measured and congruent specific absorption spectra have been published (e.g. Buiteveld et al., 1994; Kou et al., 1993; Segelstein, 1981). We assume that this spectrum is a physical constant – ignoring any variations that may be due to within-leaf chemical bonds with other molecules – and that its published values are sufficiently accurate to ignore any impact on model sensitivity. For chlorophylls and carotenoids, measured spectra in acetone or ethanol are available but with different shifts in peak absorption regions according to the polarity of the solvents. In vivo spectra have been determined by model inversion (Feret et al., 2008). These model based spectra are implicitly based on average proportions of chlorophyll a and b and the different carotenoids, while variations in these proportions can impact model sensitivity. The specific absorption spectrum for dry matter is subject to high uncertainty. The spectrum applied in multiple versions of the PROSPECT model for example, uses a constant value for wavelengths between 450 and 1200 nm which illustrates the difficulties in its estimation. In addition and analogously to chlorophylls and carotenoids, the dry matter specific absorption spectrum is a weighted average of the molecular absorption spectra of all the dry matter components of which (hemi)cellulose, lignin, starch, proteins and sugars are the major groups that are present in different relative proportions in each leaf. The impact of variations in chlorophyll and dry matter specific absorption spectra is assessed with the HDMR global sensitivity analysis as described in Section 5.1. For this purpose, DLM was extended so that the chlorophyll a and b fractions (of the total chlorophyll content) and the (hemi)cellulose, lignin, starch, sugar and protein factions (of the total dry matter content) can be used as inputs. For chlorophyll a and b, specific absorption spectra were used from Maier (2000). Although these spectra were not obtained in vivo and therefore cannot be directly used for model inversions, we assume here that their relative shapes are adequate for assessing the sensitivity to variations in chlorophyll a and b fractions. The stochastic distribution of the chlorophyll fractions is obtained from measured values in the LOPEX dataset (Hosgood et al., 1994). Spectra of different dry matter components as well as their relative distributions were obtained from Fourty et al. (1996). Considering the uncertainty of these estimated spectra, results should only be interpreted qualitatively. Fig. 6 shows an area plot of the Sobol' first order sensitivity indices for leaf absorptivity. For better visualization, all structure parameters and second order terms are grouped together. The influence of different proportions of chlorophyll a and b is almost not noticeable and is limited to a small (<1%) peak between 700 and 750 nm. In contrast, the combined sensitivity to different proportions of (hemi)cellulose, lignin, starch, sugars and proteins suggests a large effect between 700 and 1000 nm that decreases at higher wavelengths. For models where such variations cannot be taken into account, variations in the total leaf dry matter composition will increase the fraction of unexplained variance in optical properties. The NIR region in leaf absorptance spectra, although highly sensitive to total dry matter content, may thus be subject to a significant variability that cannot be explained by only considering the total leaf dry matter content. In addition to the effects of mixture compositions treated here, other factors such as shifts in specific absorption spectra may further increase the fraction of leaf optical properties that cannot be explained.

5.3. Sensitivity of model inversion to sample variability

Thus far we have assumed the measured spectra to be perfect representations of the average biochemical and structural composition. This contrasts to real measurements of leaf spectra where only a

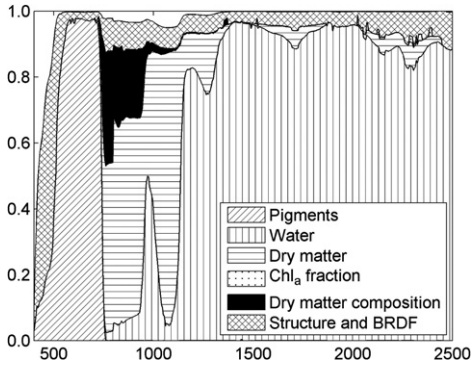

Fig. 6. Sobol' sensitivity index for absorptivity spectrum and variations in dry matter specific absorption spectrum due to differences in fractional contents of lignin, (hemi) cellulose, proteins, sugar and starch.

fraction of the leaf is sampled. In the LeuvenV dataset for example, two measurements per leaf were taken with a spot size of 10 mm. As pointed out by Castro-Esau et al. (2006), the within leaf variability in optical properties can be large compared to the between-leaf variability. This relates well to research by Rascher (2003) who demonstrated that leaves exhibit distinct spatial heterogeneity in photosynthetic efficiency. Using a single or a small number of measurements over a limited area of a leaf may lead to noticeable errors in representing average leaf optical properties. In addition, also reference measurements (spectroscopy and dry and fresh weight) are made on samples (disks) rather than on the whole leaf. The deviation between reference measurements and parameters derived from inversion may thus be significant.

Fig. 7 shows the average within-leaf standard deviation in reflectance of the measurements of the leaves in the LeuvenV dataset. Although these values are relatively small for adaxial and abaxial reflectance (<1%), their impact on the agreement between measured and predicted values of biochemical contents may be significant. The comparably large standard deviation of white reflectance in the NIR can be explained by high amounts of lateral (sideways) scattering due to the interaction of the irregular (nerves) abaxial side with an almost 100% reflecting background: a variable fraction of laterally scattered light is not captured within the sensor field of view. This was confirmed (for both measurements with integrating sphere and leaf probe) by applying different amounts of pressure between the leaf and the whitepanel. Although this effect is ignored in the following analysis, it will be instrumental in explaining observed differences in inversion accuracy in Section 6.2.

To simulate the effects of within-leaf variability, 500 reference model parameter sets were generated, each being a random draw from the distributions of chlorophyll, water, carotenoids and dry matter content in the LeuvenV dataset. Distributions of the structure

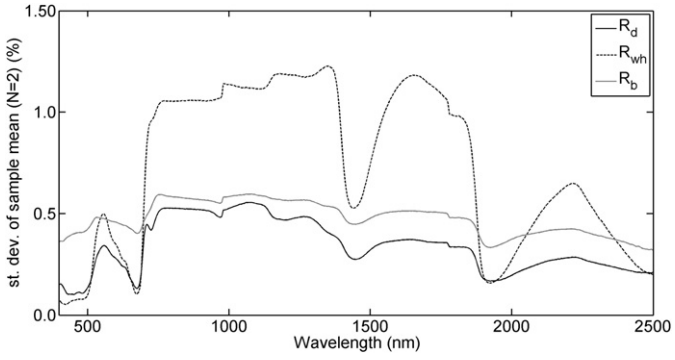

Fig. 7. Average standard deviation in measured adaxial (R_d), abaxial (R_b) and white (R_{wh}) reflectance between two samples per leaf in the Leuven dataset.

and asymmetry parameters were estimated. From each reference set, two subsets (a and b) were derived, each with small random fluctuations in their parameters to simulate the sampling effect. Within-leaf parameter distributions were adjusted to produce standard deviations in reflectance spectra approximately equal to measured values in the Leuven dataset (Fig. 7). From both subsets optical properties were simulated and combined in different inversion schemes to estimate the original parameters in the reference set. All inversion schemes are based on least squares minimization of a cost function H:

$$H = \sum_{\lambda}\left(\widehat{OP}_{a,\lambda} - OP_{a,\lambda}\right)^2 + \sum_{\lambda}\left(\widehat{OP}_{b,\lambda} - OP_{b,\lambda}\right)^2 \quad (9)$$

in which $\widehat{OP}$ denotes the modeled and OP the measured optical properties and depending on the scheme, OP_a and OP_b may stand for reflectance, transmittance or white reflectance. A constrained Nelder–Mead minimization algorithm (Nelder & Mead, 1964) was used. The four biochemical parameters and the structure parameter were estimated while other parameters were fixed at their average values (see also Section 4.5). A larger number of free parameters (e.g. including the asymmetry parameters) resulted in lower accuracies due to ill-posedness (multiple set of parameters exists that results in almost the same optical properties). Six inversion schemes were included:

- a standard inversion using the reflectance (R) from a and the transmittance (T) from b;
- an inversion in which reflectance of a and transmittance of b were combined into absorptance;
- an inversion using the mean of the white reflectance (R_{wh}) of a and b;
- three additional inversions using the previous schemes with the NIR (720–1350 nm) masked out as a rudimentary weighted least squares technique. Masking was motivated by the conclusions of Section 5.1 in which the NIR reflectance and transmittance showed almost no sensitivity to biochemical contents but high sensitivity to leaf structure.

For each biochemical content and for each scheme the root mean square error (RMSE) between reference and inverted values was calculated (Table 2). The rightmost column of the table lists the RMSE between the reference parameters and the averages of subsets a and b. This is the best possible estimate given only subsets a and b as inputs and acts therefore as a lower bound. The standard inversion scheme (column 1) using reflectance and transmittance and the full range of wavelengths has a good accuracy (compared to the optimum) for chlorophyll and water, but produces large errors for carotenoids and dry matter. This agrees with the conclusions from Feret et al. (2008) and expresses the common assumption that only chlorophyll and water contents can be accurately predicted with model inversions. Combining both spectra into absorptance does not change this conclusion although carotenoid estimations improve. Using only white reflectance leads to significant improvements that are not much larger than the lower bound. Masking of the NIR region (columns 4–6) results in a remarkable improvement in dry matter prediction and moderate improvements in carotenoid prediction for all three schemes. This sensitivity analysis marks the importance of an optimal choice of inversion schemes when combining different measurements (e.g. reflectance and transmittance) or when model inversion cannot estimate the full set of model parameters. Optimal results are not assured by the standard inversion scheme that minimizes both errors in reflectance and transmittance over the entire 400–2500 nm range. Since this analysis is entirely model-based, the conclusions do not express a lack of validity in model structure, but rather express errors inherent to sample variability and ill-posedness.

Table 2
RMSE for retrieval of biochemical parameters with different inversion schemes using simulated adaxial reflectance (R) and transmittance (T).

Scheme	R_a; T_b	R_a+T_b	$R_{w,ab}$	R_a; T_b	R_a+T_b	$R_{w,ab}$	Lower bound
Spectral range (nm)	400–2500			400–720; 1350–2500			–
Chlorophyll (g/cm^2)	5.87	5.70	5.18	6.28	6.00	6.44	4.15
Carotenoids (g/cm^2)	5.86	3.06	4.80	3.84	2.74	4.24	0.93
Water (mg/cm^2)	1.17	1.13	0.98	1.29	1.27	1.01	0.97
Dry matter (mg/cm^2)	1.79	1.72	0.56	0.73	0.71	0.43	0.39

Subscripts refer to datasets a and b. $R_{w,ab}$ is the inversion of the average white reflectance of a and b. The last column (lower bound) lists the RMSE for the average parameters of a and b compared to the reference.

6. Validation

In a first validation section the model's capabilities for approximating abaxial and adaxial reflectance and transmittance spectra of different broad-leaved species are tested and an intercalibration between DHR and BRF is made. The second subsection addresses the use of DLM in estimating biochemical content from model inversion.

6.1. Simulation of reflectance and transmittance

A model inversion procedure was set up to jointly fit measured adaxial and abaxial reflectance and transmittance of the LeuvenC dataset (20 leaves) that was collected with an integrating sphere. In a first inversion experiment, the contents of chlorophylls, carotenoids, water and dry matter, the structure parameter (f_{air}), leaf asymmetry parameters (β_{pigm}, β_{wdm} and β_{ep}), the abaxial diffusion parameter (δ) and the BRDF parameter μ were determined by the inversion procedure resulting in a ten parameter inversion. A second experiment compared these results to an inversion using default parameter values for β_{pigm}, β_{wdm}, β_{ep}, δ and μ as determined in Section 4.4 resulting in a five parameter inversion. To assess the relative improvements of a dorsiventral model over a symmetric model, the same dataset was inverted using the PROSPECT model for which simulated abaxial and adaxial optical properties are equal. The quality of the fit is expressed as the root mean squared error (RMSE) between the measured and simulated spectra.

Fig. 8 shows the agreement between measured and simulated (ten parameter inversion) adaxial and abaxial reflectance and transmittance spectra for *Citrus sinensis* L., a species with considerable differences between both faces. The fits of all four spectra show a good approximation between measured and modeled data. The largest differences are present in the NIR and around the 1850 nm water absorption region.

The statistics for all leaves are summarized in Table 3 and show that DLM is capable of representing the optical properties of the reference spectra with an average RMSE of 1.3%. The five parameter version produced overall larger fitting errors (average RMSE is 1.6%) with the largest differences in the abaxial reflectance. The inversions using PROSPECT produced for all spectra larger errors as could be expected for a symmetric model. The spectral fits using DLM in either a five or ten parameter version on combined abaxial and adaxial spectra are equal to or better than those reported in Feret et al. (2008) using the PROSPECT model on only adaxial spectra (RMSE between 1.6% and 3.9%).

An additional experiment was set up to test the theory of Section 4.3 stating that for a specified range of viewing and illumination conditions differences between DHR and BRF only depend on leaf surface structure and not on biochemical content or internal structure. This experiment used adaxial and abaxial reflectance of 12 leaves of the LeuvenC dataset taken with either integrating sphere or leaf probe. The integrating sphere measurements were inverted with a five parameter inversion scheme, identical to the scheme of Section 6.1. The leaf probe measurements were inverted with the same five parameters and the additional parameter ν required for BRF (Section 4.3). Predicted water ($R^2=0.99$), dry matter contents ($R^2=0.97$) and chlorophyll contents ($R^2=0.97$) from both datasets show a good agreement, while predicted carotenoid content had a moderate agreement ($R^2=0.76$). These observations suggest that model inversions with leaf probe and integrating sphere provide consistent results, if model structure accounts for differences between both instruments.

6.2. Parameter estimation

The performance of DLM in the estimation of biochemical contents was evaluated on both the LeuvenV and LOPEX datasets. Multiple inversion schemes are compared implementing the knowledge gathered in the sensitivity analysis (Sections 5.2 and 5.3). In addition,

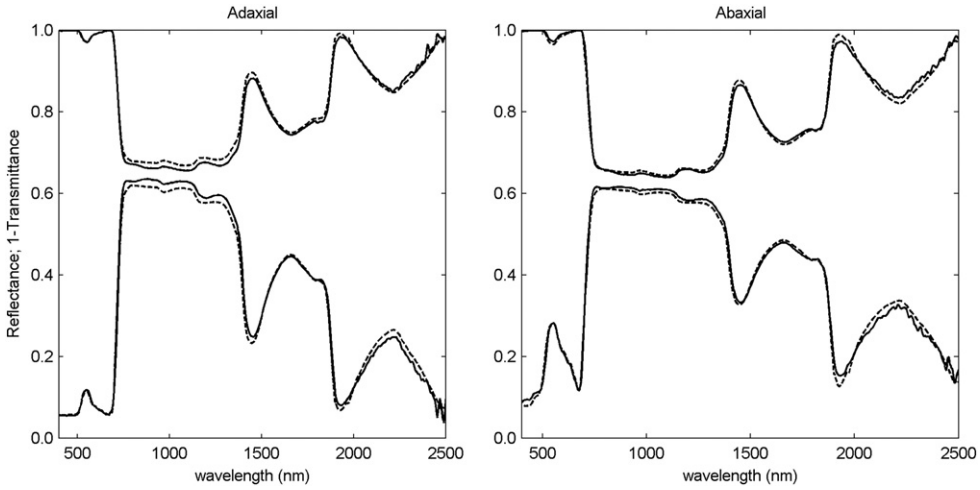

Fig. 8. Measured and simulated spectra of reflectance and transmittance for *Citrus sinensis*.

Table 3
Average and maximum RMSE (% reflectance) of the fit between measured and simulated directional–hemispherical reflectance and transmittance spectra of the LeuvenC dataset using ten and five parameter versions of DLM and PROSPECT.

	Mean RMSE (%)			Maximum RMSE (%)		
	DLM10 param.	DLM5 param.	PROSPECT	DLM10 param.	DLM5 param.	PROSPECT
Adaxial reflectance	1.25	1.59	4.22	2.04	2.88	9.48
Abaxial reflectance	1.39	1.85	6.26	2.95	4.25	10.93
Adaxial transmittance	1.02	1.14	4.82	2.29	2.4	13.06
Abaxial transmittance	1.26	1.37	4.09	2.07	2.43	9.78
Average LeuvenV	1.27	1.56	4.95	1.96	2.51	9.90

DLM is compared to PROSPECT version 5 to investigate whether the prediction of biochemical contents benefits from the use of a dorsiventral model. The four biochemical parameters and the structure parameter are included (free parameters) while for β_{pigm}, β_{wdm}, β_{ep}, δ and μ the average estimated parameters from Section 4.4 are used. For the LeuvenV dataset also ν was included. Attempts to improve the inversion by including one or more additional parameters produced lower prediction accuracies which is ascribed to over-fitting.

The LeuvenV dataset inversion schemes used combinations of adaxial reflectance, white reflectance and abaxial reflectance. For the LOPEX dataset, inversion schemes included combinations of reflectance and transmittance. For both datasets, inversions were made on either the full 400–2500 nm spectral range or with the NIR region (720–1350 nm) masked out. The headers of Tables 4 and 5 give an overview of all schemes.

The schemes and results for the LeuvenV inversion schemes are listed in Table 4. The schemes using only adaxial reflectance (schemes 1 and 2) produce good results for chlorophyll, water and dry matter, but low accuracies of carotenoids. Excluding the NIR (scheme 2) leads to a decrease in accuracy, which indicates that for content estimations from reflectance an accurate estimation of the leaf structure is required. The inversion using unweighted white reflectance (scheme 3) has a large penalty on the accuracy of the dry matter prediction while white reflectance with exclusion of the NIR (scheme 4) provided superior results, with very accurate predictions for chlorophyll, water and dry matter. The accuracy of the dry matter prediction (RMSEr = 0.4 mg/cm^2; R^2 = 0.97) is remarkable since this is traditionally assumed to be hard to estimate on fresh leaf material due to masking by water absorption (Fourty et al., 1996). The cause of the impact of the NIR on estimated dry matter accuracy may be found in different fractional constitutions of the total dry mass, that is expected to be spectrally most pronounced in the NIR (Section 5.2). In addition the large within-leaf variability of white reflectance in the NIR (Fig. 7), attributed to variable amounts of lateral scattering between the leaf and the background (see Section 5.3), may negatively impact the accuracy. Combinations of adaxial and abaxial reflectance (scheme 5) only provided results of moderate accuracy, which indicates that incorporation of abaxial reflectance, which is significantly more sensitive to leaf asymmetry, provides no additional benefits. This conclusion is in agreement with the findings of Section 5.3 since combining two spectra of different types into one inversion may degrade rather than improve results due to sampling errors. Schemes using DLM show a bias (overestimation) of the dry matter contents (RMSE > RMSEr), indicating that the dry matter specific absorption spectrum needs to be scaled when porting from PROSPECT to DLM. The accuracies using PROSPECT 5 (scheme 6) are not noticeably different from those using DLM (scheme 4), although the chlorophyll estimates are more biased while the dry matter estimates are less biased.

Table 5 lists the results of the inversions of the LOPEX dataset. Inversions using only reflectance (scheme 1) or only transmittance (scheme 2) produce good accuracies for water and moderate accuracies for dry matter. The combined use of reflectance and transmittance without band weighting (scheme 3) improves the accuracy for chlorophylls and water, but decreases the accuracy for dry matter. Excluding the NIR (scheme 4) further improves accuracy, with an important decrease in dry matter RMSEr from 1.8 to 1.1 mg/cm2. The combination of reflectance and transmittance into absorptance

Table 4
Statistics of inversion schemes for the Leuven dataset using adaxial reflectance (R_d), abaxial reflectance (T_b) and white reflectance (R_{wh}).

Scheme nr.	1	2	3	4	5	7
Model	DLM					PROSPECT 5
Spectra	R_d	R_d	R_{wh}	R_{wh}	R_d; R_b	R_{wh}
Weighting	Equal	Excl. NIR	Equal	Excl. NIR	Excl. NIR	Excl. NIRs
R^2						
Chlorophyll	0.91	0.87	0.95	0.95	0.81	0.94
Carotenoids	0.53	0.50	0.52	0.58	0.27	0.53
Water	0.90	0.86	0.90	0.94	0.87	0.92
Dry matter	0.90	0.91	0.28	0.97	0.56	0.97
RMSE regression						
Chlorophyll (g/cm^2)	5.6	6.6	4.1	4.1	9.7	4.8
Carotenoids (g/cm^2)	2.7	2.6	2.9	2.5	4.3	2.6
Water (mg/cm^2)	2.0	2.3	2.1	1.6	2.2	1.8
Dry matter (mg/cm^2)	1.0	0.9	2.5	0.4	1.9	0.5
RMSE no regression						
Chlorophyll (g/cm^2)	5.9	6.9	5.6	5.6	11.7	9.7
Carotenoids (g/cm^2)	6.0	4.7	8.4	5.9	5.8	5.5
Water (mg/cm^2)	2.0	2.3	2.5	1.7	2.3	2.0
Dry matter (mg/cm^2)	2.0	1.7	3.0	1.7	3.2	0.8
RMSE spectrum fit	0.5%	0.5%	1%	0.8%	1.2%	0.8%

Table 5
Statistics of inversion schemes for the LOPEX dataset using spectra (adaxial) reflectance (R) and transmittance (T).

Scheme nr.	1	2	3	4	5	6
Model	DLM					PROSPECT 5
Spectra	R	T	R; T	R; T	$R+T$	$R+T$
Weighting	Equal	Equal	Equal	Excl. NIR	Excl. NIR	Excl. NIR
R^2						
Chlorophyll	0.41	0.46	0.57	0.58	0.63	0.64
Water	0.91	0.90	0.94	0.95	0.93	0.95
Dry matter	0.64	0.69	0.49	0.81	0.80	0.80
RMSE regression						
Chlorophyll (g/cm^2)	14.1	15.6	12.4	11.9	11.1	11
Water (mg/cm^2)	2.1	2.7	1.7	1.7	1.8	1.8
Dry matter (mg/cm^2)	1.5	1.4	1.8	1.1	1.1	1.2
RMSE no regression						
Chlorophyll (g/cm^2)	15.0	15.6	12.4	12.7	11.3	11.0
Water (mg/cm^2)	2.4	2.9	1.8	1.8	1.8	1.8
Dry matter (mg/cm^2)	2.2	2.6	4.7	3.1	3.6	3.8
RMSE spectrum fit	0.9%	0.9%	1.4%	1.2%	1.9%	1.8%

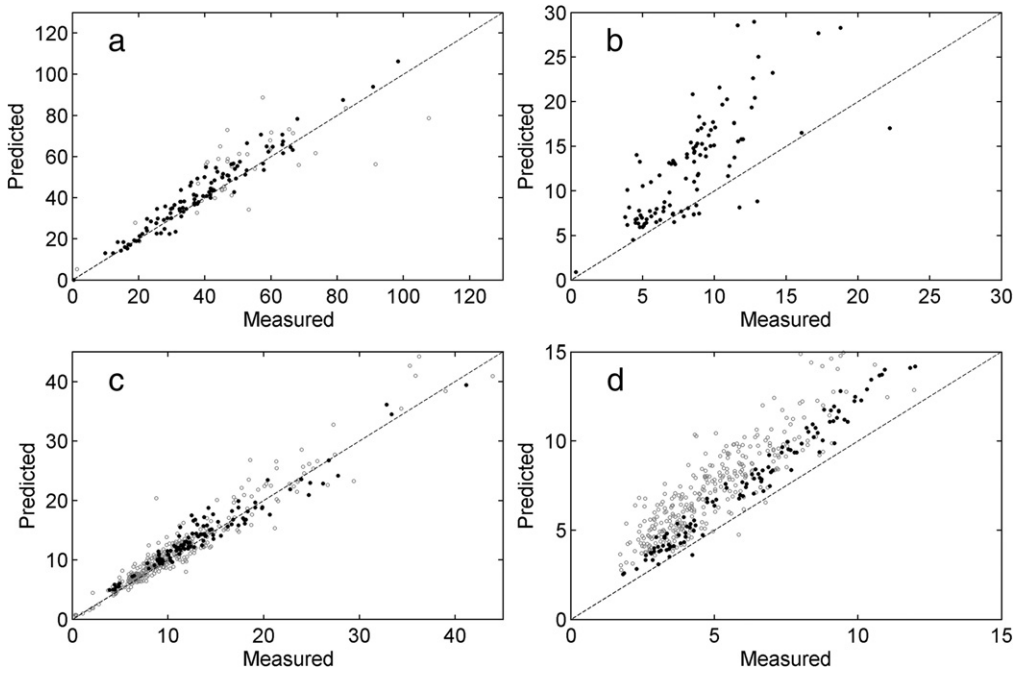

Fig. 9. Comparison between measured and predicted contents of (a) chlorophylls (μg/cm), (b) carotenoids (μg/cm), (c) water (mg/cm) and (d) dry matter (mg/cm) using DLM with parameters from Table 6. (● Leuven, ○ LOPEX).

(scheme 5) provides no clear benefit. The PROSPECT 5 scheme produced almost equal accuracies.

For Tables 4 and 5, the bottom line lists the RMSE of reflectance or transmittance of the fit of the measured on the predicted spectrum. For none of the inversion schemes could this value be related to the accuracy of biochemical content estimates, indicating that improvements in approximating the exact shape of reflectance or transmittance curves may not necessarily lead to a better prediction of leaf biochemistry.

Care should be taken when directly comparing the LOPEX results to the Leuven results. The coefficients of determination should not be compared since they also reflect the variability of the dataset (parameter range), but RMSE values can be compared. The overall accuracies for the predicted water contents are almost equal to the Leuven dataset. The LOPEX accuracies for chlorophyll are significantly lower which may be caused by errors in pigment extraction procedures as reported by Feret et al. (2008). This result agrees with the lower accuracies reported by Jacquemoud et al. (1996) and Feret et al. (2008). The accuracy of dry matter contents is comparable to schemes 1 and 2 of the Leuven dataset that use only adaxial reflectance.

Fig. 9 shows scatter-plots of the measured and predicted values of the four inverted components for the best inversion schemes on both datasets and Table 6 lists extended statistics for these schemes. Two additional parameters were included: the water content as fraction of the total leaf fresh weight and the ratio of chlorophylls to carotenoids. The fraction of water can be estimated with a very high accuracy for both datasets. This also indicates that prediction errors for water and dry matter may be correlated. The low accuracy of the car/chl ratio on the other hand may limit the usability of the carotenoids estimates in biochemical applications. The slope of the regression indicates the bias in the prediction which is acceptable for chlorophyll and water contents. The dry matter content is overestimated (slope<1) for both the LeuvenV and LOPEX datasets, which indicates that its specific absorption spectrum should be scaled. The same applies to the carotenoid estimates of the LeuvenV dataset. Note that only measured values of the water specific absorption spectrum are available, while other spectra (dry matter, carotenoid and chlorophyll) are determined by inversion procedures and can therefore be model dependent (specific absorption spectra were used from the PROSPECT 5 model). Differences in biases between both datasets may be explained in procedural differences in content estimations (e.g. pigment extraction, weighting).

Table 6
Extended statistics for the best inversion schemes for the Leuven and LOPEX datasets.

Dataset	Leuven	LOPEX
Spectra	R_{wh}	$R+T$
Weighting	Excl. NIR	Excl. NIR
# parameters	6	5
R^2		
Chlorophyll	0.95	0.63
Carotenoids	0.58	
Water	0.94	0.93
Dry matter	0.97	0.80
Car/Chl ratio	0.24	
Fraction of water	0.98	0.93
Slope regression		
Chlorophyll	0.92	1.04
Carotenoids	0.62	
Water	0.97	1.00
Dry matter	0.81	0.63
Car/Chl ratio	0.93	
Fraction of water	1.04	1.16
RMSE regression		
Chlorophyll (g/cm^2	4.1	11.1
Carotenoids (g/cm^2)	2.5	
Water (mg/cm^2)	1.6	1.8
Dry matter (mg/cm^2)	0.4	1.1
Car/Chl ratio (–)	6.4%	
Fraction of water (%)	2.4%	4.1%
RMSE no regression		
Chlorophyll (g/cm^2)	5.6	11.3
Carotenoids (g/cm^2)	5.9	
Water (mg/cm^2)	1.7	1.8
Dry matter (mg/cm^2)	1.7	3.5
Car/Chl ratio (–)	6.7%	
Fraction of water (%)	3.7%	10%
RMSE spectrum fit	0.8%	1.9%

Knowledge gathered from the inversion of leaf optical models can also be applied to the inversion of canopy radiative transfer models. Although governed by different processes, the principles of band weighting and alternative methods to combine different (multi-angular) reflectance spectra may significantly improve the retrieval of canopy biochemistry and structure parameters.

The comparable performance of DLM and PROSPECT 5 on both datasets may imply that no large gains in accuracy are to be expected by introducing more sophisticated models that provide a better representation of leaf internal structure. In explanation of these results, the implicit inclusion of leaf asymmetry into the PROSPECT 5 model (Section 4.7) via the refractive index as an effective parameter can be pointed out. An explicit treatment of leaf asymmetry as is provided by DLM may however become an important factor when a further breakdown of pigments (e.g. chlorophyll a and b) or dry matter (e.g. lignin, cellulose, sugars…) is targeted.

7. Conclusions

In this research, the impact of leaf asymmetry on radiative transfer was modeled and investigated. A dorsiventral leaf model was introduced that considers the asymmetric distribution of pigments, water and dry matter. The differences in light diffusion between adaxially and abaxially incident collimated light are modeled by introducing an abaxial diffusion parameter. Both adaxial and abaxial reflectance and transmittance of a wide variety of leaves can be accurately simulated with good precision. The precise simulations of optical properties of both faces may facilitate improvements in canopy radiative transfer modeling, since dorsiventral properties of leaves can have a significant impact on canopy reflectance. Continued research efforts are required to evaluate this potential.

The sensitivity analysis focused on optimizing the model inversion process. Results indicate that parameter estimation from model inversion may be improved by (i) combining reflectance and transmittance measurements to minimize the impact of leaf structure (ii) adjusting procedures to account for variability in the dry matter specific absorption spectrum and (iii) inversion schemes that minimize the impact of sampling errors. The white reflectance was found to exhibit favorable qualities making it a suitable candidate to replace reflectance and transmittance measurements for parameter estimations.

Knowledge gathered in the sensitivity analysis was applied in different model inversion schemes to retrieve pigment, water and dry matter content for two independently collected datasets, LeuvenV (2008, abaxial, adaxial and white reflectance) and LOPEX (1994, reflectance and transmittance). For the LeuvenV dataset, the white reflectance measure returned the most accurate estimates for all four parameters, provided the NIR (720–1350 nm) was excluded from the inversion process. Additional knowledge on the leaf abaxial reflectance could not improve these estimates. Inversions of the LOPEX dataset demonstrated that by excluding the NIR significant improvements in the estimation of leaf dry matter can be achieved. Overall accuracies for water and dry matter contents in LOPEX were equal to the accuracies in the Leuven dataset for equal inversion schemes. Combinations of two spectra of a different type into a single inversion did not improve accuracies, as was predicted in the sensitivity analysis. The good accuracies for dry matter content estimation may encourage attempts breaking down the total dry matter estimates into cellulose, lignin, protein, sugar and starch components. No impact on content prediction accuracy was found by the use of biconical reflectance measurements instead of DHR. The major improvements in content predictions were found by procedures that account for sampling errors, uncertainly in the specific absorption spectra and variability in specular reflectance rather than by the use of a more sophisticated (dorsiventral) model structure.

Since DLM is designed for broad-leaved species, no tests were performed on coniferous needle-shaped leaves, although the dorsiventral structure of some species with differentiated mesophyll such as *Abies* sp. (Johnson et al., 2005) may prove to be compatible.

DLM has important potential in the study of leaf radiative transfer while it can also be used to relate anatomic differences causing asymmetric scattering and absorption to evolutionary and ontological strategies of plants to optimize the interaction with their light environment.

Acknowledgments

Funding support for this project has been provided by the K.U. Leuven as part of the Special Research Fund program OT04047. The Authors are grateful to the Joint Research Center, Institute for Remote Sensing Applications of the European Commission for freely providing the LOPEX dataset and to professors Stéphane Jacquemoud (Institut de Physique de Globe de Paris & Université Paris Diderot) and Christophe François (Laboratoire Ecologie, Université Paris-Sud) for valuable comments on the model construction.

Appendix A. Supplementary data

Supplementary data associated with this article can be found, in the online version, at doi:10.1016/j.rse.2009.07.014.

References

Allen, W., Gausman, H., Richardson, A., & Thomas, J. (1969). Interaction of isotropic light with a compact plant leaf. *Journal of the Optical Society of America*, *59*(10), 1376−1379.

Allen, W., Gausmann, H., & Richardson, A. (1970). Mean effective optical constants of cotton leaves. *Journal of the Optical Society of America*, *60*, 542−547.

Ashikhmin, M., & Shirley, P. (2000). An anisotropic phong BRDF model. *Journal of Graphics Tools*, *5*, 25−32.

Atzberger, C. (2004). Object-based retrieval of biophysical canopy variables using artificial neural nets and radiative transfer models. *Remote Sensing of Environment*, *93*, 53−67.

Bacour, C., Baret, F., Béal, D., Weiss, M., & Pavageau, K. (2006). Neural network estimation of LAI, fAPAR, fCover and LAIxCab, from top of canopy MERIS reflectance data: Principles and validation. *Remote Sensing of Environment*, *105*, 313−325.

Baldini, E., Facini, O., Nerozzi, F., Rossi, F., & Rotondi, A. (1997). Leaf characteristics and optical properties of different woody species. *Trees*, *12*(2), 73−81.

Baranoski, G. V. (2006). Modeling the interaction of infrared radiation (750 to 2500 nm) with bifacial and unifacial plant leaves. *Remote Sensing of Environment*, *100*(3), 335−347.

Bjõrck, A. (1996). *Numerical methods for Least Squares problems.* Philadelphia, Penn: SIAM books.

Bousquet, L., Lachérade, S., Jacquemoud, S., & Moya, I. (2005). Leaf BRDF measurements and model for specular and diffuse components differentiation. *Remote Sensing of Environment*, *98*(2–3), 201−211.

Buiteveld, H., Hakvoort, J. M. H., & Donze, M. (1994). The optical properties of pure water, in Ocean Optics XII. In J. S. Jaffe (Ed.), *Proc. SPIE, vol. 2258*. (pp. 174−183).

Castro-Esau, K., Sanchez-Azofeifa, G., Rivard, B., Wright, S., & Quesada, M. (2006). Variability in leaf optical properties of Mesoamerican trees and the potential for species classification. *American Journal of Botany*, *93*(4), 517−530.

Cook, R., & Torrance, K. (1981). A reflectance model for computer graphics. *Computer Graphics*, *15*, 307−316.

Cui, M., Vogelmann, T., & Smith, W. (1991). Chlorophyll and light gradients in sun and shade leaves of *Spinacia oleracea*. *Plant, Cell and Environment*, *14*, 493−500.

Dawson, T., Curran, P., & Plummer, S. (1998). LIBERTY — modeling the effects of leaf biochemical concentration on reflectance spectra — Pigments of photosynthetic biomembranes. *Remote Sensing of Environment*, *65*(1), 50−60.

Evans, L., Albury, K., & Jennings, N. (1996). Relationships between anatomical characteristics and ozone sensitivity of leaves of several herbaceous dicotyledonous plant species at Great Smoky Mountains national park. *Environmental and Experimental Botany*, *36*, 413−420.

Feret, J. B., François, C., Asner, G. P., Gitelson, A. A., Martin, R. E., Bidel, L. P., et al. (2008). PROSPECT-4 and 5: Advances in the leaf optical properties model separating photosynthetic pigments. *Remote Sensing of Environment*, *112*(6), 3030−3043.

Fourty, T., Baret, F., Jacquemoud, S., Schmuck, G., & Verdebout, J. (1996). Leaf optical properties with explicit description of its biochemical composition: Direct and inverse problems. *Remote Sensing of Environment*, *56*(2), 104−117.

Govaerts, Y., Jacquemoud, S., Verstraete, M., & Ustin, S. (1996). Three-dimensional radiation transfer modeling in a dicotyledon leaf. *Applied Optics*, *35*(33), 6585−6598.

Habel, R., Kusternig, A., & Wimmer, M. (2007). Physically based real-time translucency for leaves. Rendering Techniques 2007. *Proceedings Eurographics Symposium on Rendering* (pp. 253−263).

Hosgood, B., Jacquemoud, S., Andreoli, G., Verdebout, J., Pedrini, A., & Schmuck, G. (1994). Leaf Optical Properties EXperiment 93 (LOPEX93). *Technical report, Joint*

Research Centre, Institute for Remote Sensing Applications, Unit for Advanced Techniques, TP 272, Ispra (VA), Italy.
Jacquemoud, S., & Baret, F. (1990). PROSPECT: A model of leaf optical properties spectra. *Remote Sensing of Environment*, *34*(2), 75—91.
Jacquemoud, S., & Ustin, S. (2001). Leaf Optical Properties: A state of the art. *8th International Symposium of Physical Measurements & Signatures in Remote Sensing*.
Jacquemoud, S., Verdebout, J., Schmuck, G., Andreoli, G., & Hosgood, B. (1995). Investigation of leaf biochemistry by statistics. *Remote Sensing of Environment*, *54*(3), 180—188.
Jacquemoud, S., Ustin, S. L., Verdebout, J., Schmuck, G., Andreoli, G., & Hosgood, B. (1996). Estimating leaf biochemistry using the PROSPECT leaf optical properties model. *Remote Sensing of Environment*, *56*(3), 194—202.
Johnson, D., Smith, W., Vogelmann, T., & Brodersen, C. (2005). Leaf architecture and direction of incident light influence mesophyll fluorescence profiles. *American Journal of Botany*, *92*, 1425—1431.
Knapp, A., Vogelmann, T., McClean, T., & Smith, W. (1988). Light and chlorophyll gradients within Cucurbita cotyledons. *Plant, Cell and Environment*, *11*, 257—263.
Kou, L., Labrie, D., & Chylek, P. (1993). Refractive indices of water and ice in the 0.65–2.5 μm spectral range. *Applied Optics*, *32*, 3531—3540.
Kubelka, P. (1954). New contributions to the optics of intensely light-scattering materials. Part II: Nonhomogeneous layers. *Journal of the Optical Society of America*, *44*, 330—335.
Kuusk, A. (1991). Determination of vegetation canopy parameters from optical measurements. *Remote Sensing of Environment*, *37*, 207—218.
Lichtenthaler, H. K. (1987). Chlorophylls and Carotenoids: Pigments of Photosynthetic Biomembranes. *Methods in Enzymology*, *148*, 350—382.
Lillesaeter, O. (1982). Spectral reflectance of partly transmitting leaves: Laboratory measurements and mathematical modeling. *Remote Sensing of Environment*, *12*, 247—254.
Ma, K., Baret, F., Barroy, P., & Bousquet, L. (2007). A leaf optical properties model accounting for differences between the two faces. *10th International Symposium on Physical Measurements and Signatures in Remote Sensing, 2007. ISPMSRS07*. International Society for Photogrammetry and Remote Sensing.
Maier, S. (2000). Modeling the radiative transfer in leaves in the 300 nm to 2.5 um wavelength region taking into consideration chlorophyll fluorescence. The leaf model SLOPE. Ph.D. thesis, Technische Universität München, Oberpfaffenhofen (Germany).
McCain, D., Croxdale, J., & Markley, J. (1993). The spatial distribution of chloroplast water in *Acer platanoides* sun and shade leaves. *Plant, Cell and Environment*, *16*, 727—733.
Merzlyak, M. N., Melo, T., & Naqvi, K. R. (2004). Estimation of leaf transmittance in the near infrared region through reflectance measurements. *Journal of Photochemistry and Photobiology. B, Biology*, *74*, 145—150.
Nelder, J., & Mead, R. (1964). A simplex method for function minimization. *Computer Journal*, *7*, 308—313.
Oppenheim, A., & Schafer, R. (1989). *Discrete-time signal processing.* Prentice-Hall.
Pääkkönen, E., Holopainen, T., & Kärenlampi, L. (1995). Ageing-related anatomical and ultrastructural changes in leaves of birch (*Betula pendula* Roth.) clones as affected by low ozone exposure. *Annals of Botany*, *75*, 285—294.
Rascher, U. (2003). Imaging and imagining spatiotemporal variations of photosynthesis of simple leaves. *Nova Acta Leopoldina*, *88*(332), 367—380.
Richter, T., & Fukshansky, L. (1996). Optics of a bifacial leaf: 1. A novel combined procedure for deriving the optical parameters. *Photochemistry and Photobiology*, *63*(4), 507—556.
Schaepman-Strub, G., Schaempan, M., Painter, T., Dangel, S., & Martonchik, J. (2006). Reflectance quantities in optical remote sensing — Definitions and case studies. *Remote Sensing of Environment*, *103*, 27—42.
Segelstein, D.J. (1981). The complex refractive index of water. Master's thesis, Department of Physics. University of Missouri-Kansas City.
Sims, D. A., & Gamon, J. A. (2002). Relationships between leaf pigment content and spectral reflectance across a wide range of species, leaf structures and developmental stages. *Remote Sensing of Environment*, *81*(2–3), 337—354.
Sobol', I. (2001). Global sensitivity indices for nonlinear mathematical models and their Monte Carlo estimates. *Mathematics and Computers in Simulation*, *55*, 271—280.
Stuckens, J., Somers, B., Delalieux, S., Verstraeten, W. W., & Coppin, P. (2009). The impact of common assumptions on canopy radiative transfer simulations: A case study in Citrus orchards. *Journal of Quantitative Spectroscopy and Radiative Transfer*, *110*, 1—21.
Taiz, L., & Zeiger, E. (2006). *Plant physiology*, fourth edition Sunderland, Massachusetts: Sinauer Associates.
Vogelmann, T., & Martin, G. (1993). The functional significance of palisade tissue: Penetration of directional versus diffuse light. *Plant, Cell and Environment*, *16*, 65—72.
Vogelmann, T. C., Bornman, J. F., & Yates, D. J. (1996). Focusing of light by leaf epidermal cells. *Physiologia Plantarum*, *98*(1), 43—56.
Woolley, J. (1971). Reflectance and transmittance of light by leaves. *Plant Physiology*, *47*, 656—662.
Yamada, N., & Fujimura, S. (1991). Nondestructive measurement of chlorophyll pigment content in plant leaves from three-color reflectance and transmittance. *Applied Optics*, *30*, 3964—3973.
Zarco-Tejada, P., Miller, J., Pedrùos, R., Verhoef, W., & Berger, M. (2006). FluorMODgui V3.0: A graphic user interface for the spectral simulation of leaf and canopy chlorophyll fluorescence. *Computers & Geosciences*, *32*, 577—591.
Ziehn, T., Hughes, K., Griffiths, J., Porter, R., & Tomlin, A. (2009). A software tool for global sensitivity analysis of complex models. *Environmental Modelling & Software*, *24*, 775—785.